Int. J. Electrochem. Sci., 14 **(2019)** 6247 – 6256, doi: 10.20964/2019.07.09

International Journal of
ELECTROCHEMICAL
SCIENCE
www.electrochemsci.org

Effects of pH on the Electrochemical Behavior and Stress Corrosion Cracking of X80 Pipeline Steel in Simulated Alkaline Soil Solution

Ping Liang[*], *Yier Guo, Hua Qin, Yanhua Shi, Fei Li, Lan Jin, Zheng Fang*

School of Mechanical Engineering, Liaoning Shihua University, Fushun 113001, China
[*]E-mail: liangping770101@163.com

Received: 12 February 2019 / *Accepted:* 18 April 2019 / *Published:* 10 June 2019

The electrochemical behavior of X80 pipeline steel in alkaline soil solution with different pH value was studied by mean of potentiodynamic polarization and electrochemical impedance spectroscopy (EIS). The results of electrochemical measurements showed that the general corrosion and pitting corrosion resistance of X80 pipeline steel increased with increasing pH, which could be attributed to formation of a protective $FeCO_3$ film in the solution (pH ≥11.0). Stress corrosion cracking susceptibility decreased with increasing pH during the slow strain rate tensile tests. The pits were found to be an important factor in the initiation of transgranular cracks below pH=10.0. However, when pH>10, intergranular cracking occurred because of selective dissolution at grain boundaries

Keywords: X80 Pipeline Steel, pH, General Corrosion, Pitting Corrosion, Stress Corrosion Cracking

1. INTRODUCTION

It has been reported that the main deterioration mechanism of structural integrity of the buried pipeline steel in soils was the external corrosion of pipe, including general corrosion, crevice corrosion [1], pitting corrosion as well as stress corrosion cracking (SCC) [2-5]. These resulted in a great uncertainty to the service safety of buried pipelines. A synergistic system of protective organic coatings and cathodic protection (CP) has been identified as the most effective method [6] to avoid or reduce the external corrosion. However, a disbonded coating from pipeline was visible due to the combined effect of the degradating organic coatings and CP [7], which leaded to a local electrochemical environment, to be different from that in soils[8]. Previous researches [9-11] have pointed out that the pH change of the solution in disbonded region occurred, and this also caused some localized corrosion behavior. For example, SCC, a type of localized corrosion, was a vital threat to the safe operation of the natural gas pipelines[12]. It has been recognized as the high-pH SCC and the near-neutral pH SCC

for buried pipeline steels according to the pH of soil [13, 14]. In addition, pitting corrosion of pipeline was affected by the soil pH [15, 16].

The low carbon microalloyed X80 pipeline steel, which was a fairly new steel, was used as pipeline material in China and other countries [17]. The material had used widely for building the gas transmission pipelines, which is due to its high-intensity and high-toughness [18, 19]. Ku'erle region (Xinjiang province, Northwest China) produces abundant natural gas, where a great number of gas pipelines have been buried. And some of gas pipelines buried were corroded including general corrosion, pitting and SCC easily occurred in this area [20]. Therefore, studies on the effects of pH on the corrosion behavior of X80 steel were essential for the application of the steel under soil environmental

In this study, the general corrosion and pitting corrosion behaviors of X80 steel in Ku'erle soil solution over a range of pH values, which simulated the pH of disbonded coating from pipeline steel, were instudied by polarization curves; moreover, the SCC susceptibility was also evaluated by the slow strain rate technique (SSRT), and the fracture micrographs were obtained using scanning electron microscope (SEM), and the ultimate aim was to provide some references for the engineering applications of X80 steel in soils environment.

2. EXPERIMENTAL

2.1 Test material and test solution

X80 pipeline steel was used as the test material in this paper. Its chemical composition (wt.%) is given in Table 1.

Table 1. Chemical compositions of X80 pipeline steel (wt.%)

C	Mn	P	S	Si	Cu	Al	Ti	Cr
0.041	1.67	0.010	0.0006	0.196	0.258	0.042	0.011	0.031
Ca	Pb	Sb	Sn	As	B	Ni	Nb	Fe
0.0017	0.0028	0.0031	0.0048	0.007	0.003	0.246	0.095	Bal.

Soil samples of Ku'erle region were collected from three representative sites where lots of pipelines were buried. Table 2 shows the chemical compositions of the simulated Ku'erle soil solution, whose pH was adjusted from 8.0 to 11.0 with sulfuric acid (H_2SO_4) or sodium hydroxide (NaOH). The solutions ware purged with nitrogen gas for 2 h prior to the test, and the solutions were remained purging throughout all the slow strain rate tensile (SSRT) tests. Experiments in soil solutions with ph=9 have been studied in my previous papers, so in this paper will be compared with it [20].

Table 2. Chemical compositions of simulated Ku'erle soil solution (g / L)

Compounds	$NaHCO_3$	KNO_3	Na_2SO_4	$CaCl_2$	NaCl	$MgCl_2 \cdot 6H_2O$
Concentration	0.1462	0.2156	2.5276	0.2442	3.1707	0.6699

2.2 Potentiodynamic polarization and electrochemical impedance spectroscopy measurements

The electrochemical experiments were performed in a three-electrode cell system, which includes a saturated calomel electrode (SCE) as a reference electrode and a platinum sheet as a counter electrode. All potential values in this paper were referred to SCE.

In order to stabilize the surface, the specimens were immersed in the deoxygenated simulated solutions with various pH at open circuit potential (OCP) for 0.5 h. Polarization curve was acquired using PAR 2273 potentiostat at a scanning rate of 20 $mV \cdot min^{-1}$.

Electrochemical impedance spectroscopy (EIS) measurements were carried out using EG&G 2273 with the AC amplitude of the sinusoidal perturbation of 10 mV and the measurement frequency from 100 kHz down to 10 mHz. Z view software version 3.20 was used for the data fitting.

2.3 Slow strain rate tensile tests (SSRT)

The stress cracking corrosion susceptibility of X80 pipeline steel in simulated soil solution with various pH was studied using SSRT method. Tests were obtained on flat tensile specimens (gauge length: 32 mm, gauge thickness: 2 mm, and gauge width: 6 mm). The gauge lengths of the specimens were polished with emery paper from 200 to 1000, then degreased with acetone in an ultrasonic cleaner, followed by washing with distilled water and finally dried in air. The strain rate was controlled at 1×10^{-6} s^{-1}. The SCC susceptibility was expressed in terms of the percentage change in the reduction in area (RA) and the fracture time (t_f). The lower the RA and the t_f, the higher the SCC susceptibility. RA was calculated from the following equation:

$$RA=\frac{S_0 - S_A}{S_0}\times 100\% \quad (1)$$

where S_0 is the initial area of the tensile specimen, and S_A the final fracture area of the tensile specimen.

After SSRT tests, the fracture surfaces of various samples were observed using scanning electron microscope (SEM).

3. RESULTS & DISCUSSION

3.1 Effects of pH on the electrochemical behavior

The potentiodynamic polarization of curves for X80 pipeline steel in simulated alkaline soil solution at various pH values were measured and are shown in Figure 1. Figure 2 gives the fitted data of corrosion current densities (i_{corr}) in four kinds of solutions. It could be seen that, as the pH increased from 8.00 to 11.00, the corrosion potential increased from -732 mV to -663 mV, while the corrosion

current density (i_{corr}) decreased from 6.287 μA·cm^{-2} to 0.312 μA·cm^{-2}, respectively. The increase in corrosion potential and the decrease of i_{corr} in high-pH (pH ≥11.0) solutions were believed to arise from the differences in surface films (i.e., corrosion product).

From the compositions of the simulated alkaline soil solution, as listed in Table 2, it may be deduced that two possible electrochemical reactions occurred in the range of pH as following equations:

$$Fe + 2H_2O \rightarrow Fe(OH)_2 + 2H^+ + 2e \quad (2)$$

$$Fe + HCO_3^- \rightarrow FeCO_3 + H^+ + 2e \quad (3)$$

It had been report that when the pH fell within a range of 8.2 to 9.5, the equation (2) was the main reaction [21], and the HCO_3^- ion had less or no effect on the surface corrosion product, thus, $Fe(OH)_2$ was favored on the surface, which was a layer of metastable film and less protective [22], and this probably caused a worse corrosion resistance.

The second reaction (Eq.(2)) was dependent on pH and HCO_3^- [23]. When the pH of the soil solution was relatively high (pH ≥11.0), the HCO_3^- ion was dominate, and a stable ferrous carbonate ($FeCO_3$) film was easily formed on the specimen surface[24]. The white-gray film observed on the specimens polarized in pH=11.0 solution provided evidence of $FeCO_3$ formation [15]. Moreover, with increasing pH, the concentration of OH^- was increased, which caused a more $FeCO_3$ and Cr_2O_3 in the passive film because of the following reaction(Eq.4-6) [25], the $FeCO_3$ and Cr_2O_3 inhibited the dissolution of X80 pipeline steel and reduced obviously the corrosion current density. Therefore, an increasing tendency of resistance to general corrosion was exhibited with the enhancement of pH.

$$Cr \rightarrow Cr^{3+} + 3e^- \quad (4)$$

$$Cr^{3+} + 3OH^- \rightarrow Cr(OH)_3 \quad (5)$$

$$Cr(OH)_3 \rightarrow Cr_2O_3 + 3H_2O \quad (6)$$

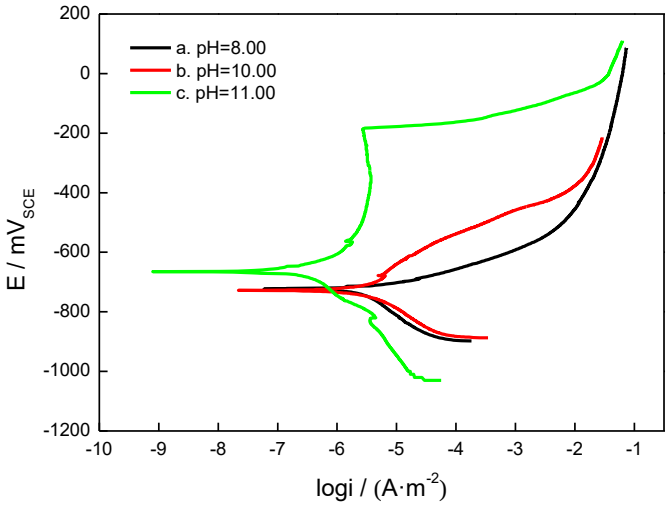

Figure 1. Potentiodynamic polarization curves of X80 pipeline steel in alkaline soil simulated solutions with different pH levels.

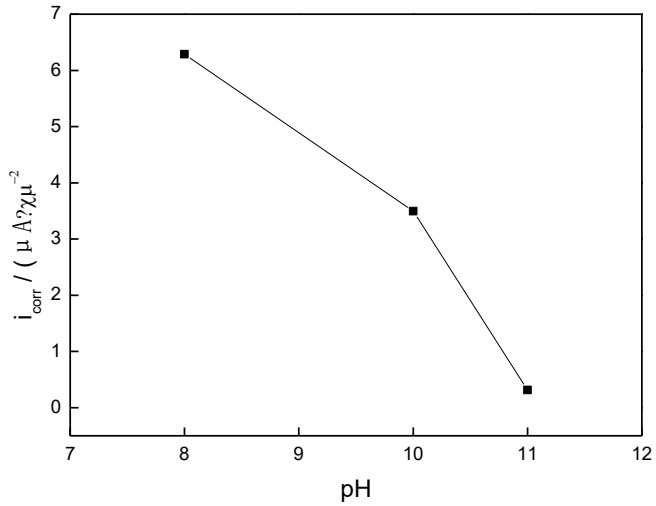

Figure 2. Effects of pH on the i_{corr} of X80 pipeline steel in alkaline soil simulated solutions

3.2 Electrochemical impedance spectroscopy measurements (EIS)

Figure 3 demonstrates the measured EIS results for X80 pipeline steel in four solutions. For all the samples, the EIS plots consisted of capacitive loop in the frequency range. There was the smallest diameter of the semicircle impedance arc at pH=8.0, while it was the biggest at pH =11.0.

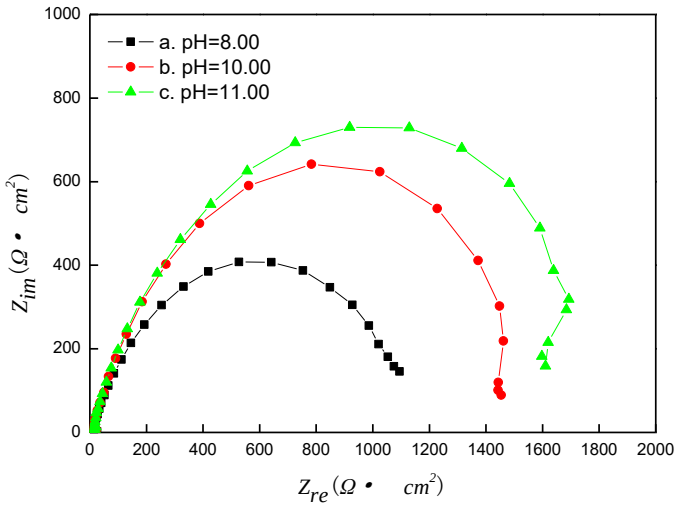

Figure 3. EIS plots measured on X80 pipeline steel in simulated soil solution with various pH

An electrical equivalent circuit $R_s(QR_t)$ is applied to model the EIS data for the specimens, where R_s, R_t and Q are solution resistance, charge-transfer resistance and constant phase element (CPE) for the double-charge layer, respectively. Figure 4 depicts the changes in the R_t of X80 pipeline steel in these solutions with various pH values. The R_t value reflected the resistance of the ionic migration across the surface film [26]. In this figure, the R_t increased with increasing solution pH values, implying the low pH had the higher activity than the high pH, and a more protective film was formed in the solution with pH 11.0, which acted as a barrier for penetration of corrosion species, and then decreased the further

dissolution of pipeline steel through a surface block effect [27], which was beneficial to the general corrosion resistance. Good correlation was obtained between the results of potentiodynamic polarization curves and EIS measurements.

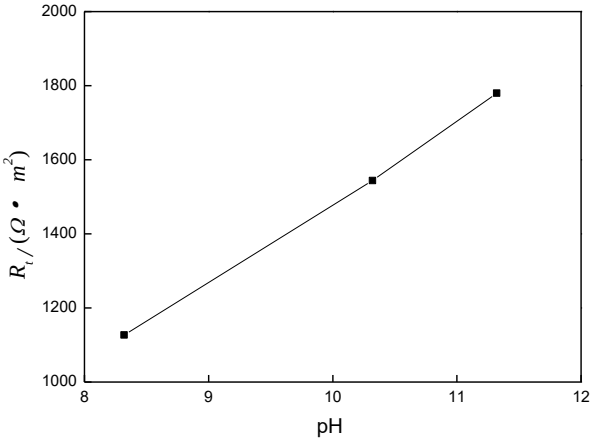

Figure 4. *Variation of charge transfer resistance (R_t) as a function of pH in simulated soil solution*

3.3 Effects of pH on pitting corrosion

In addition, it was obvious from Figure 1 that the width of passive potential region was narrowed and the pitting potential (E_{pit}) lowered as the pH decreased, which revealed that the pitting susceptibility increased as the decreasing solution pH.

Optical micrographs of the surfaces obtained after polarization experiments in four solutions are shown in Fig.5. It was clear that the number of pits increased with decreasing solution pH, while there were fewer and smaller pits in pH =11.00 solution. Since the ratio of HCO_3^- ions to Cl^- ions was relatively high at pH ≥11.0 solution, the decreased pitting susceptibility with increasing pH was caused by the protective $FeCO_3$ film. In contrast, in a low pH solution, pitting susceptibility was obviously increased because there was no apparent carbonate product deposited and its resultant surface block effect, and the aggressive environment caused by the increased ratio of Cl^- ions. In this case, once pitting initiated, pits may be the localized acid environmental conditions and facilitated the initiation of SCC in the specimens.

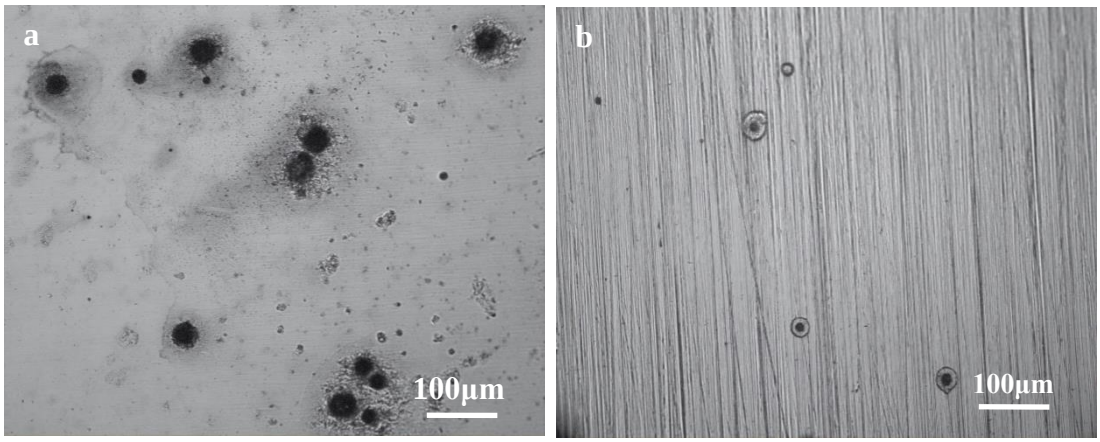

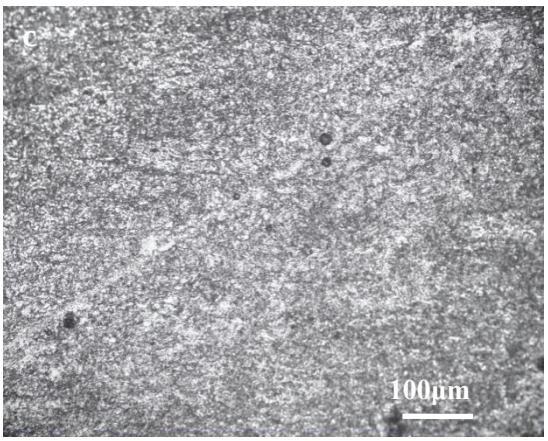

Figure 5. Optical photographs of the surface of X80 pipeline steel after polarization experiments in four kinds of solutions with various pH: (a) pH=8.00, (b) pH=10.00, and (c) pH=11.00

3.4 Effect of pH on stress corrosion cracking

The stress-strain curves of X80 pipeline steel in air and in soil solutions with various pH values at the open circuit potentials (OCPs) are exhibited in Figure 6. The effects of pH on the reduction in area (RA) and fracture time (t_f) are also illustrated in Fig.7. As can be seen, both RA and t_f were lower in these alkaline solutions than in air for the corresponding specimens, which implied that X80 pipeline steel was susceptible to environmentally assisted cracking in these solutions. Moreover, it was found that the values of the two parameters at pH 11.0 were larger than that at pH 8.0. The SCC susceptibility was the higher in the lower pH of the soil solutions.

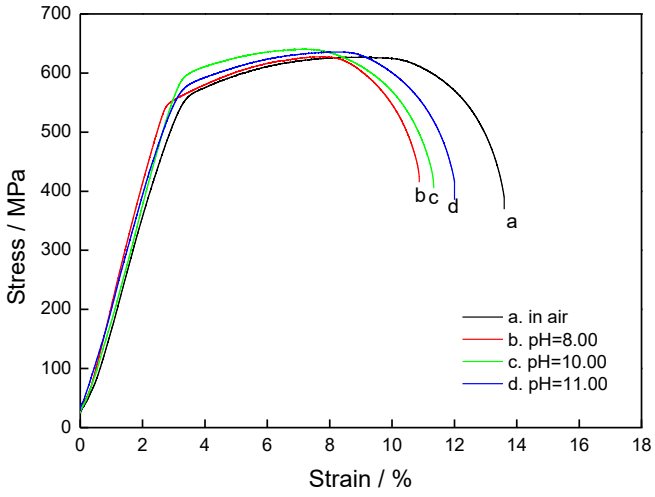

Figure 6. Stress-strain curves of X80 steel obtained in simulated alkaline soil solution with various pH

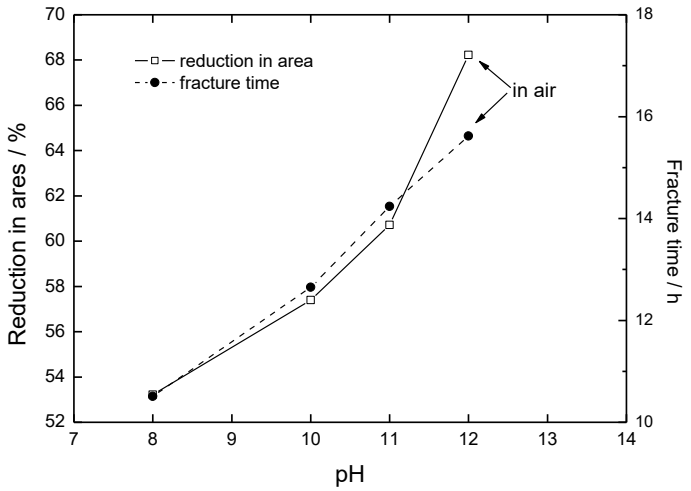

Figure 7. Effects of solution pH on RA and fracture time(t_f)

After SSRT in the soil solutions, the fracture surfaces were observed by means of a scanning electron microscope (SEM), as presented in Figs.8a-d. The fracture surface in air was characterized by the presence of a great number of dimples, as illustrated in Fig. 8(a), which indicated a ductile behavior.

Fig. 8(b) reveals that X80 pipeline steel specimen exposed to solution with pH 8.00 showed a quasi-cleavage and transgranular stress corrosion crack (TGSCC) failure, and the TGSCC was also found pH 10.00, respectively. In addition, it appeared that the cracks initiated from the corrosion pits when the pH increased from 8.00 to 10.0, as shown in Fig. 8(d). This was because that the aggressive Cl^- ions were the dominant species in relatively low pH soil solutions, which easily induced a lot of pits, as shown in Figs. 5(a)-(c). Thus, pitting caused local acidification within corrosion pits, and the local acidification environment could facilitate some of the reactions involved in the crack initiation and growth process. Therefore, pitting seemed to have played a significant role in the transgranular stress corrosion cracking in the pH range from 8.0 to 10.0 for the simulated soil solution.

However, the stress corrosion cracking path of the specimen exposed to the relative high-pH solution (pH≥11.0) was intergranular, as presented in Fig. 8(c). It is generally known that [28, 29] the film rupture and anodic metal dissolution at the crack tip are responsible for this form of SCC. In the soil solution (pH=11.00), a $FeCO_3$ protective film was formed, which may strongly cling to the crack sides and effectively prevented anodic dissolution on the insusceptible cracking path. Thus, a sufficient passivity to allow selective dissolution at grain boundaries and hence promoted SCC by providing a susceptible cracking path [30]. As a result, stress corrosion cracks in high-pH solution propagated along the grain boundaries, indicating an occurrence of intergranular stress corrosion cracking (IGSCC). All of the results show that the pH of soil solution impact the SCC behavior, and the SCC susceptibility of X80 pipeline steel in the simulated soil solution was increased by low pH.

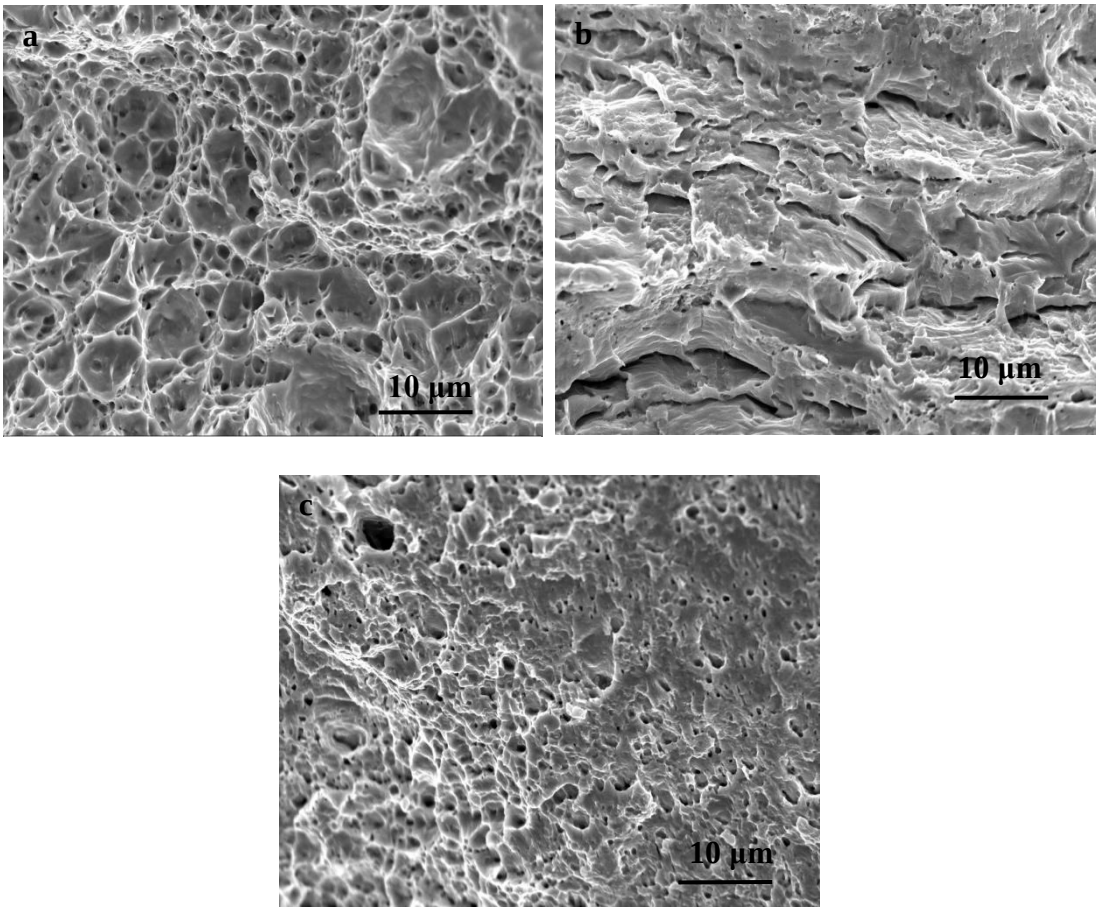

Figure 8. Fracture surface morophologies of X80 pipeline steel after SSRT testing in alkaline simulated soil solution with different pH values: (a) in air, (b) pH=8.00, (c) pH=11.00

4. CONCLUSIONS

(1) In the simulated alkaline soil solution, X80 pipeline steel displayed a higher corrosion rate for general corrosion and a lower breakdown potential ($E_{pitting}$) for pitting with decreasing pH, which was inferred that a gradually decreased pH exerted a detrimental effect on the pipeline steel because the formation of a protective film in a relatively low pH solution was more difficult.

(2) When the pH of simulated alkaline soil solution was relatively low, pitting corrosion obviously occurred due to the Cl^- ion attack from the optical photograph observation, and pits was to be a susceptible site for transgranular stress corrosion cracking initiation and propagation. However, when the pH of the simulated alkaline soil solution was above 11.0, the SCC propagated along the grain boundaries because of the formation of a protective $FeCO_3$ film, which allowed a selective dissolution at grain boundaries and hence leaded to IGSCC.

ACKNOWLEDGEMENTS

The authors are grateful for the financial support from the Natural Science Foundation of Department of Science ＆Technology of Liaoning Province (registration number: 20180550348).

References

1. Z.F. Li, F.X. Gan, X.H. Mao, *Corros. Sci.,* 44(2002)689
2. G.V. Boven, W. Chen, R. Rogge, *Acta. Mater.,* 55(2007)29
3. A. Contreras, A. Albiter, M. Salazar, R. Pérez, *Mat. Sci. Eng. A-Struct.,* 407(2005)45
4. B.W. Pan, X. Peng, W.Y. Chy, Y.J. Su, L.J. Qiao, *Mat. Sci. Eng. A-Struct.,* 434(2006)76
5. M. Hattori, H. Suzuki,Y. Seko, K. Takai, *Jom,* 69(2017)1375
6. T. Kamimura, H. Kishikawa. *Corrosion,* 54(1998)979
7. J.L. Luo, C.J. Lin, Q. Yang, S.W. Guan, *Prog. Org. Coat.,* 31(1997)289
8. M.C. Yan, J.Q. Wang, E.H. Han, W. Ke, *Corros. Sci.,* 50(2008)1331
9. J.J. Perdomo, I. Song. *Corros. Sci.,* 42(2000)1389
10. J.J. Perdomo, I. Song. *Corros. Sci.,* 43(2001)515
11. L. Fan, Z.Y. Liu, W.M. Guo, J. Hou, C.W. Du, X.G. Li, *Acta. Metall. Sin-Engl.,* 28(2015)866
12. M. Zhu, C.W. Du, X.G. Li, Z.Y. Liu, S.R. Wang, T.L. Zhao, J.H. Jia, *J. Mater. Eng. Perform.,* 23(2014)1358
13. J.Q. Wang, A. Atrens, *Corros. Sci.,* 45(2003)2199
14. W. Chen, S.H. Wang, R. Chu, F. King, T.R. Jack, R.R. Fessler, *Metall. Mater. Trans. A, 34*(2003)2601
15. X. Mao, X. Liu, R.W. Revie, *Corrosion,* 50(1994)651
16. W.M. Zhao, T.M. Zhang, R.F. Xin, M.M. Wang, H. Ai, J.B. Sun, Y. Wang, *J. Therm. Spray. Techn.,* 24(2015)974
17. J.D. Kang, W.Y. Zheng, D. Bibby, B.S. Amirkhiz, J. Li. *J. Mater. Eng. Perform.,* 25(2016)227
18. K. Banerjee, U.K. Chatterjee, *Scripta. Mater.,* 44(2001)213
19. F. Xie, D. Wang, M. Wu, C.X. Yu, D.X. Sun, X. Yang, C.H. Xu, *Metall. Mater. Trans. A,* 49(2018)1372
20. P. Liang, X.G. Li, C.W. Du, X. Chen, *Mater. Design,* 30(2009)1712
21. X. Liu, X. Mao, *Scripta. Mater.,* 33(1995)145
22. Y.M. Zeng, J.L. Luo, P.R. Norton, *Electrochim. Acta.,* 49(2004)703
23. J.J, Park, S.I. Pyun, K.H. Na, S.M. Lee, Y.T. Kho, *Corrosion,* 58(2002)329
24. F. Xie, D. Wang, C.X. Yu, Y. Zong, M. Wu, *Int. J. Electrochem. Sci.,* 12(2017)9565
25. N.S. Bharasi, M.G. Pujar, C. Mallika, U.K. Mudali, *T. Indian. I. Metals.,* 70(2017)1953
26. L.W. Wang, X.G. Li , C.W. Du, P. Zhang, Y.Z. Huang, *J. Iron Steel. Res. Int.,* 22(2015)135
27. M.C. Li, Y.F. Cheng, *Electrochim. Acta,* 53(2008)2381
28. Y.F. Cheng, M. Wilmott, J.L. Luo, *Appl. Surf. Sci.,* 152(1999)161
29. R.N. Parkins, *Corrosion,* 52(1996)363
30. A.K. Pilkey, S.B. Lambert, A. Plumtree, *Corrosion,* 51(1995)91